

Parameter-Free Clustering via Self-Supervised Consensus Maximization (Extended Version)

Lijun Zhang^{1*}, Suyuan Liu^{1*}, Siwei Wang², Shengju Yu¹, Xueling Zhu³,
Miaomiao Li⁴, Xinwang Liu^{1†}

¹College of Computer Science and Technology, National University of Defense Technology, Changsha, 410073, China

²Academy of Military Sciences, Beijing, 100091, China

³Xiangya Hospital, Central South University, Changsha, 410008, China

⁴School of Computer, Changsha College, Changsha, 410022, China

{junliz, suyuanliu, wangsiwei13}@nudt.edu.cn, yu-shengju@foxmail.com, zhuxueling@csu.edu.cn,
miaomiaolinudt@gmail.com, xinwangliu@nudt.edu.cn

Abstract

Clustering is a fundamental task in unsupervised learning, but most existing methods heavily rely on hyperparameters such as the number of clusters or other sensitive settings, limiting their applicability in real-world scenarios. To address this long-standing challenge, we propose a novel and fully parameter-free clustering framework via Self-supervised Consensus Maximization, named SCMax. Our framework performs hierarchical agglomerative clustering and cluster evaluation in a single, integrated process. At each step of agglomeration, it creates a new, structure-aware data representation through a self-supervised learning task guided by the current clustering structure. We then introduce a nearest neighbor consensus score, which measures the agreement between the nearest neighbor-based merge decisions suggested by the original representation and the self-supervised one. The moment at which consensus maximization occurs can serve as a criterion for determining the optimal number of clusters. Extensive experiments on multiple datasets demonstrate that the proposed framework outperforms existing clustering approaches designed for scenarios with an unknown number of clusters.

Code — <https://github.com/ljz441/2026-AAAI-SCMax>

Main Paper — Processing

Introduction

Clustering is a fundamental machine learning task that aims to partition unlabeled data into groups based on intrinsic similarities (Zhang et al. 2025a; Zhou et al. 2025; Liu et al. 2024; Yu et al. 2024; Qin and Qian 2024; Wang et al. 2024). As a typical unsupervised learning method, clustering has been widely applied in various domains such as image processing (Qiu et al. 2024; Zhang et al. 2024), and text analysis (He, Wang, and Zhang 2025; Yang et al. 2025), serving as a crucial tool for understanding data structures.

*These authors contributed equally.

†Corresponding author.

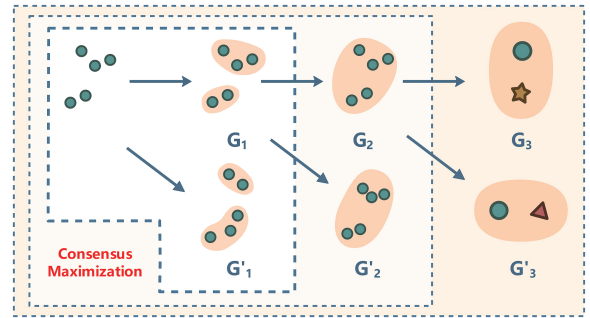


Figure 1: Motivation of Consensus Maximization. Here, G_i and G'_i denote the cluster structures from original and self-supervised representations, respectively. The optimal structure is determined when their consensus is maximized. For simplicity, each type of shape in G_3 and G'_3 is represented as a class set.

However, existing clustering methods often heavily rely on hyperparameters such as the number of clusters or other sensitive settings, which poses significant challenges when dealing with tasks involving open and complex data structures. Unlike supervised learning, clustering lacks the guidance of class labels and, in real-world applications, it is generally infeasible to preset any priors. This reality has driven the emergence of parameter-free clustering techniques. In recent years, numerous clustering methods that do not rely on predefined cluster numbers or other sensitive settings have been proposed, including density-based (Abbas, El-Zoghbi, and Shoukry 2021; Rodriguez and Laio 2014), graph-based (Sun et al. 2024; Peng et al. 2019; Shah and Koltun 2017), hierarchy-based (Yang and Lin 2025; Dang et al. 2021; Sarfraz, Sharma, and Stiefelagen 2019), and probabilistic model-based (Wang et al. 2022; Yang et al. 2019) approaches. Among them, hierarchy-based methods have become a prominent research direction due to their ability to naturally generate multi-level cluster structures during the clustering process, thereby producing multiple candidate values of K with strong interpretability.

Although current parameter-free hierarchical clustering methods attempt to address the core issue of K -value selection, they do not entirely eliminate the reliance on priors. Many such methods, while not explicitly specifying K , introduce other sensitive parameter settings, such as distance thresholds or probability cutoffs, which still require manual tuning and can affect the stability and generalizability of the clustering results. Overall, these methods can typically be divided into two stages: cluster number generation and cluster structure evaluation. In the generation stage, common strategies often adopt split-and-merge techniques (Ronen, Finder, and Freifeld 2022; Liu et al. 2023; Dai et al. 2024). However, these approaches usually imply assumptions about the initial number of clusters and can only explore a limited set of K values in practice, making it difficult to cover all potential clustering structures. In the evaluation stage, common techniques such as the elbow method (Shi et al. 2021; Schubert 2023) often rely on smoothed or ambiguous evaluation curves that require manually defined thresholds or subjective identification of "elbow points," which can be unstable in high-dimensional or complex data scenarios. Therefore, how to automatically generate and evaluate cluster structures without any prior knowledge or manual settings remains a key challenge in achieving truly parameter-free clustering.

To address the above issues, we propose a fully parameter-free clustering framework via Self-supervised Consensus Maximization, named SCMax. Falling under the category of hierarchical clustering, SCMax achieves the complete process from cluster number generation to cluster structure evaluation without relying on any prior settings. Specifically, in the generation stage, SCMax constructs nearest neighbor graphs to guide the cluster merging process and automatically produces a set of candidate cluster structures. Unlike existing methods, SCMax does not assume an initial number of clusters or restrict the search space, enabling the direct and efficient generation of multiple candidates and significantly reducing the K -value search space. Furthermore, based on the principle of nearest neighbor stability, we design a Nearest Neighbor Consensus (NNC) evaluation metric to measure the agreement of merging decisions between the original and self-supervised feature representations. The optimal number of clusters is automatically determined at the point of consensus maximization. Compared to traditional methods, this metric avoids reliance on subjective parameters such as thresholds or elbow points. The entire process is fully automated, achieves strong generalization and robustness, and embodies the essence of "parameter-free" clustering. The motivation is illustrated in Fig. 1. The main contributions of this work are summarized as follows.

- We propose a fully parameter-free clustering framework that performs hierarchical agglomerative clustering and cluster evaluation in a single integrated process. This framework does not require any hyperparameters of the number of clusters or other sensitive settings.
- We design a cluster evaluation metric based on nearest neighbor consensus, which measures the agreement between the nearest neighbor-based merge decisions derived from the original and self-supervised representa-

tions. The moment at which consensus maximization occurs can serve as a criterion for determining the optimal number of clusters.

- Extensive experiments on multiple datasets demonstrate that the proposed framework outperforms existing clustering approaches designed for scenarios with an unknown number of clusters.

Related Work

This section focuses on the branch of hierarchical clustering under the umbrella of parameter-free clustering, with particular emphasis on two key aspects: cluster number generation and cluster structure evaluation.

Cluster Number Generation

Within the framework of parameter-free clustering, traditional hierarchical clustering methods mainly adopt two types of cluster number generation strategies: bottom-up and top-down. The former, such as agglomerative clustering (Li et al. 2024; Xing et al. 2021), starts with a larger number of clusters and progressively merges the most similar ones; the latter, such as divisive clustering (Bagirov, Aliguliyev, and Sultanova 2023; Liu et al. 2023; Dai et al. 2024), begins with fewer clusters and recursively splits them into smaller sub-clusters. In addition, some methods combine the strengths of both approaches, such as split-and-merge strategy (Zhao, Yang, and Deng 2024; Xiao et al. 2023; Ronen, Finder, and Freifeld 2022), which dynamically decides whether to split or merge clusters based on an initial assumption of the number of clusters. While these methods are capable of constructing a hierarchical structure of clustering results, they still face several practical challenges. On one hand, many of them heavily rely on the initial number of clusters. If this initial value deviates significantly from the true number of clusters, it may lead to inefficient clustering or misguide the subsequent structural exploration, resulting in poor candidate cluster structures. On the other hand, most approaches require a predefined search space for the number of clusters in order to avoid the high computational cost of brute-force enumeration, which inevitably limits their flexibility and generalization ability.

To address these challenges, Nearest Neighbor Clustering (NN clustering) methods have attracted increasing attention in recent years (Yang and Lin 2025; Dang et al. 2021; Sarfraz, Sharma, and Stiefelhagen 2019). Compared to traditional strategies, NN clustering offers superior computational efficiency, with complexity reduced to $O(N \log N)$. Without the need to assume an initial number of clusters or constrain the search space, NN clustering can directly and efficiently generate multiple candidate cluster structures, significantly reducing the K -value search space. These methods not only improve runtime performance and clustering quality but also scale well to large datasets, demonstrating broad applicability in hierarchical clustering tasks.

Cluster Structure Evaluation

In hierarchical clustering frameworks, the core challenge of parameter-free clustering lies in how to automatically iden-

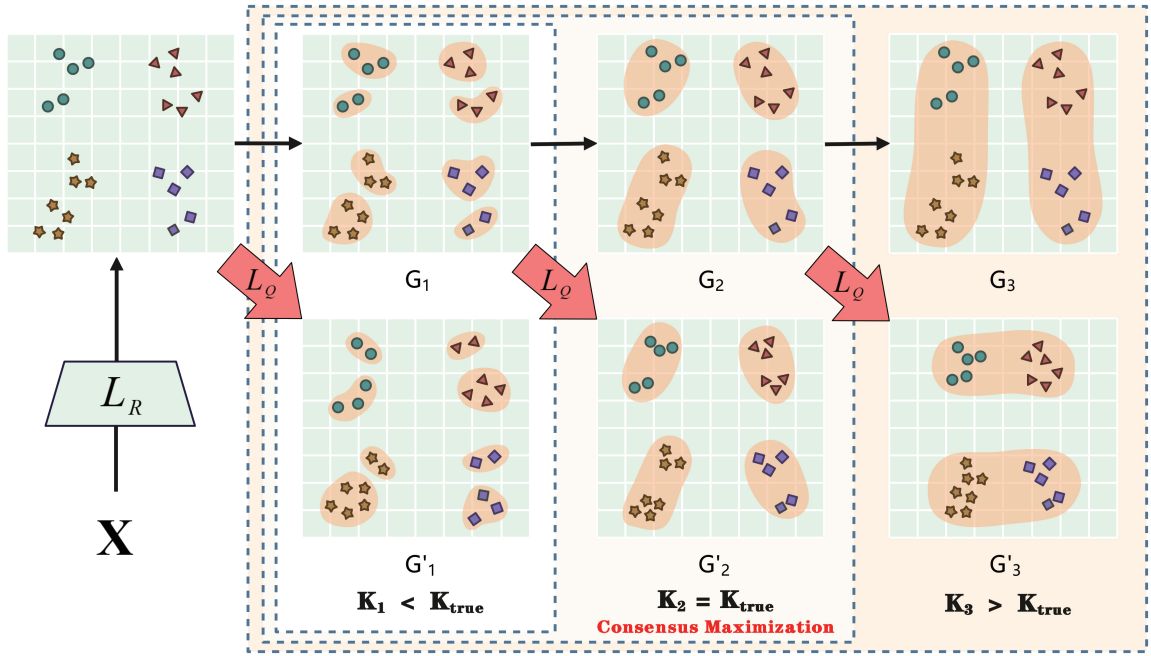


Figure 2: The proposed SCMax framework.

tify the optimal partition from a set of hierarchical candidate cluster structures, which is crucial for ensuring clustering performance. Traditional approaches such as the Elbow Method (Kodinariya and Makwana 2013; Shi et al. 2021; Schubert 2023) typically rely on manually set thresholds or visually identified inflection points to determine when to stop the clustering process. However, such methods are often highly sensitive to subjective settings, lack adaptive capabilities, and are vulnerable to noise, which can lead to unstable and unreliable evaluation results.

To overcome these limitations, we observe a phenomenon referred to as nearest-neighbor stability in the actual feature representation space and propose a nearest-neighbor consensus-based cluster structure evaluation metric. This metric measures the consistency of nearest-neighbor merging decisions between the original features and those obtained via self-supervised learning. The moment when this consensus maximization occurs corresponds to the optimal cluster structure. This metric is entirely free of manually set hyperparameters and can adaptively capture the intrinsic structure of the data, enabling truly parameter-free, stable, and reliable cluster structure evaluation.

Methodology

In this section, we propose a fully parameter-free clustering framework termed SCMax. The overall framework is illustrated in Fig. 2.

Autoencoder Module

Given a dataset $\mathbf{X} \in \mathbb{R}^{N \times D}$, where N denotes the number of samples and D denotes the feature dimension. For the original features \mathbf{X} , there may exist redundancy and noise.

Therefore, we use an autoencoder to nonlinearly map \mathbf{X} into a customizable feature space to extract more representative feature embeddings. Specifically, we denote the encoder and decoder as $E(\mathbf{X}, \theta)$ and $D(\mathbf{X}, \phi)$, where θ and ϕ are network parameters. Based on this, the mapped L -dimensional latent feature representation is $\mathbf{Z} = E(\mathbf{X}) \in \mathbb{R}^{N \times L}$, and the reconstructed representation is $\hat{\mathbf{X}} = D(E(\mathbf{X}))$. The reconstruction loss between input \mathbf{X} and output $\hat{\mathbf{X}}$ is denoted as L_R . Thus, the autoencoder’s loss is formulated as:

$$L_R = \sum_{i=1}^N \|\mathbf{X}_i - \hat{\mathbf{X}}_i\|_2^2. \quad (1)$$

Cluster Number Generation Module

Based on the dimensionally reduced feature representation \mathbf{Z} , we begin cluster number generation. In SCMax, we adopt nearest neighbor merging to generate cluster candidates due to its efficiency, as it aggregates data using only local neighbor relations without constructing a global distance matrix. The resulting partitions have been shown to closely match true clusters and perform well across various tasks (Sarfranz, Sharma, and Stiefelhagen 2019; Dang et al. 2021; Yang and Lin 2025). Specifically, each sample is initially treated as an individual cluster, forming the first-level cluster structure. We then recursively merge these clusters, where at each step, each cluster performs merging operations guided by the nearest neighbor graph, thereby generating a new cluster structure. To efficiently construct the nearest neighbor graph, we employ an approximate nearest neighbor search method (i.e., KD-Tree). Each cluster is represented by the mean of its sample vectors, and the nearest class neighbors are computed based on these mean vectors. Unlike

sample-level nearest neighbor merging, this approach performs merging at the class level, which simplifies computation and maintains a complexity of $O(K \log K)$, where K denotes the number of clusters. We denote the nearest neighbor graph as $\mathbf{A} \in \mathbb{R}^{K \times 1}$. Given the integer indices \mathbf{A} representing the nearest neighbor of each class, we can construct a symmetric adjacency matrix $\mathbf{G} \in \mathbb{R}^{K \times K}$ in linear time as follows:

$$\mathbf{G}(i, j) = \begin{cases} 1, & \text{if } j = \mathbf{A}_i \text{ or } \mathbf{A}_j = i \text{ or } \mathbf{A}_i = \mathbf{A}_j \\ 0, & \text{otherwise} \end{cases}, \quad (2)$$

where \mathbf{A}_i and \mathbf{A}_j denote the nearest neighbors of classes i and j , respectively. The adjacency matrix \mathbf{G} captures the inter-class relationships, and its connected components correspond to the resulting clusters. Since \mathbf{G} describes class-level relations, a reverse label mapping is required to propagate the clustering results back to the sample level, thereby obtaining the final cluster label vector $\mathbf{Q} \in \mathbb{R}^{N \times 1}$. This clustering formulation is extremely simple and parameter-free, directly producing a set of candidate cluster structures from the data.

Cluster Structure Evaluation Module

After obtaining multiple hierarchical candidate cluster structures \mathbf{G} , the core problem of the evaluation module is how to select the optimal clustering structure from these candidates. Before formally introducing the cluster structure evaluation module in SCMax, we first need to introduce the core concept of “nearest neighbor stability.” Specifically, when perturbations are applied to the representation \mathbf{Z} , the adjacency relationships of classes in the nearest neighbor graph may change. We define the degree of change in nearest neighbor graph structure before and after perturbation as the classes’ nearest neighbor stability, which indicates the robustness of the local structure to perturbations.

Next, we provide the definition and implementation of the perturbation. In SCMax, perturbations are not based on random noise but are implemented by introducing label \mathbf{Q} -based contrastive constraints. These constraints impose structural interventions on the fixed feature representation \mathbf{Z} , indirectly altering the adjacency relationships among classes to simulate perturbations. Under the contrastive learning constraint, we aim to pull together samples of the same class while pushing apart samples from different classes. Hence, we define the following structural contrastive loss:

$$L_Q = \frac{1}{|\mathcal{P}|} \sum_{(i,j) \in \mathcal{P}} \mathbf{D}_{ij} - \frac{1}{|\mathcal{N}|} \sum_{(i,j) \in \mathcal{N}} \mathbf{D}_{ij}, \quad (3)$$

where $\mathcal{P} = \{(i, j) \mid q_i = q_j, i \neq j\}$ denote the set of positive (same-class) sample pairs, $\mathcal{N} = \{(i, j) \mid q_i \neq q_j\}$ denote the set of negative (different-class) sample pairs, and \mathbf{D}_{ij} represents the Euclidean distance between z_i and z_j , where $\mathbf{D} \in \mathbb{R}^{B \times B}$ and B is the batch size. To avoid $O(N^2)$ complexity in computation, SCMax does not perform full-sample contrastive learning but adopts a mini-batch training strategy. That is, at each training step, a local Euclidean distance matrix is constructed within the current batch, significantly reducing computation and memory costs. This loss

function uses label \mathbf{Q} as supervision to guide the fixed representation \mathbf{Z} to undergo structured changes in semantic space, achieving the perturbation goal. Unlike random noise perturbations, this method’s intervention in local structure is directional and controllable, effectively influencing nearest neighbor stability and providing a clean and explicit baseline for subsequent cluster structure evaluation.

At this point, after perturbing the fixed representation \mathbf{Z} under the guidance of cluster labels \mathbf{Q} , we obtain a set of new self-supervised representations $\mathbf{Z}' = \{\mathbf{Z}'_1, \mathbf{Z}'_2, \dots, \mathbf{Z}'_i\}$, where each \mathbf{Z}'_i corresponds to the perturbation guided by \mathbf{Q}_i . Based on the fixed representation \mathbf{Z} , we find the nearest neighbors within each class in \mathbf{G}_i and perform merging to get the next cluster structure \mathbf{G}_{i+1} . Similarly, based on the self-supervised representation \mathbf{Z}'_i , we find the nearest neighbors in \mathbf{G}_i and merge to obtain a new cluster structure \mathbf{G}'_{i+1} . So far, we have two sets of cluster structures: $\mathbf{G} = \{\mathbf{G}_1, \mathbf{G}_2, \dots, \mathbf{G}_i\}$ from the fixed representation \mathbf{Z} , and $\mathbf{G}' = \{\mathbf{G}'_2, \dots, \mathbf{G}'_i\}$ from the self-supervised representation \mathbf{Z}' . By measuring the consistency between the merging decisions of nearest neighbors executed on the original representation \mathbf{Z} and the self-supervised representation \mathbf{Z}' —that is, the similarity between cluster structures \mathbf{G}_i and \mathbf{G}'_i —we define the Nearest Neighbor Consensus (NNC) metric as follows:

$$\text{NNC}(\mathbf{G}_i, \mathbf{G}'_i) = \max_{\pi \in \mathcal{S}} \frac{1}{N} \sum_{j=1}^N \mathbf{1}(\mathbf{Q}_i(j) = \pi(\mathbf{Q}'_i(j))), \quad (4)$$

where \mathbf{Q}_i and \mathbf{Q}'_i denote the cluster assignment labels for each sample in the clusters \mathbf{G}_i and \mathbf{G}'_i , respectively; the indicator function $\mathbf{1}(\cdot)$ returns 1 if the condition is true and 0 otherwise; π represents the set \mathcal{S} of all possible label mappings under the Hungarian algorithm for label alignment.

Finally, we provide an in-depth discussion and analysis of the NNC metric, explaining why the moment when consensus reaches its maximum corresponds to the optimal clustering structure. The detailed process is illustrated in the Fig. 2.

- **When the cluster number K_i corresponding to \mathbf{G}_i is greater than the true cluster number:** perturbations applied on the fixed representation \mathbf{Z} at the previous step significantly affect the nearest neighbor relationships among intra-class samples of the true cluster structure. Since samples in true clusters are close to each other, even slight perturbations can break the original adjacency relations, indicating unstable nearest neighbor relations at K_{i-1} . Consequently, the nearest neighbor graph constructed from the perturbed self-supervised representation \mathbf{Z}' significantly differs from that constructed from \mathbf{Z} , resulting in low similarity between \mathbf{G}_i and \mathbf{G}'_i .
- **When K_i equals the true cluster number:** perturbations applied on \mathbf{Z} at the previous step do not significantly affect intra-class adjacency. At this point, K_{i-1} approaches the true cluster number, with most intra-class samples merged into the same cluster, greatly reducing the number of intra-class nearest neighbors and leading to a stable adjacency relationships. Therefore, the difference between perturbed and original nearest neighbor

Algorithm 1: SCMax

- 1: **Input:** Dataset $\mathbf{X} \in \mathbb{R}^{N \times D}$
- 2: **Output:** Cluster number K^* , cluster labels \mathbf{Q}^*
- 3: Compute latent representation $\mathbf{Z} \in \mathbb{R}^{N \times L}$ by Eq.(1)
- 4: Initialize each sample as a singleton cluster
- 5: Get \mathbf{G}_1 via nearest neighbor merging on \mathbf{Z} by Eq.(2)
- 6: Derive K_1, \mathbf{Q}_1 from connected components in \mathbf{G}_1
- 7: Let $i = 1$
- 8: **while** at least three clusters exist in \mathbf{G}_i **do**
- 9: Update \mathbf{G}_{i+1} via nearest neighbor merging based on \mathbf{Z} by Eq.(2)
- 10: Obtain K_{i+1} and \mathbf{Q}_{i+1} by computing connected components in \mathbf{G}_{i+1}
- 11: Generate perturbed representation \mathbf{Z}' based on \mathbf{Q}_i by Eq.(3)
- 12: Compute \mathbf{G}'_{i+1} via nearest neighbor merging based on \mathbf{Z}' by Eq.(2)
- 13: Compute NNC score between \mathbf{G}_{i+1} and \mathbf{G}'_{i+1} by Eq.(4)
- 14: Record $K_{i+1}, \mathbf{Q}_{i+1}$ and corresponding NNC score
- 15: $i \leftarrow i + 1$
- 16: **end while**
- 17: Select K^*, \mathbf{Q}^* with the highest NNC score
- 18: **return** K^*, \mathbf{Q}^*

graphs is minimal, and the similarity between \mathbf{G}_i and \mathbf{G}'_i reaches its maximum.

- **When K_i is less than the true cluster number:** perturbations applied on \mathbf{Z} disrupt the inter-class boundary structure of the true cluster. Since true clusters usually have certain gaps, perturbations blur or overlap these gaps, causing samples from different true clusters to be incorrectly grouped together. This breaks the original inter-class boundaries, making nearest neighbor relations unstable again at K_{i-1} . As a result, the difference between perturbed and original nearest neighbor graphs becomes significant again, and the similarity between \mathbf{G}_i and \mathbf{G}'_i decreases.

In summary, when the nearest neighbor consensus reaches its maximum, the corresponding cluster structure \mathbf{G}^* precisely reflects the optimal cluster distribution of the data, and the corresponding cluster number K^* and label set \mathbf{Q}^* can be regarded as the final clustering result. It can be seen that the proposed NNC metric does not depend on any prior hyperparameters and can adaptively evaluate the intrinsic structure of the data.

Computational Complexity Analysis

The pseudo-code of SCMax is presented in Algorithm 1. This subsection focuses on analyzing the main computational and memory overheads. Regarding time complexity, constructing the class-level nearest neighbor index using a KD-Tree for K classes requires $O(K \log K)$ time. The symmetric adjacency matrix \mathbf{G} is then constructed in linear time, $O(K)$. To assess local consistency, SCMax computes the Euclidean distance matrix within each mini-batch of size

Dataset	Samples	Dimension	Cluster
MSRCv1	210	1302	7
HW2	2000	784	10
Wiki	2866	10	10
MNIST	5000	784	10
Cifar10	50000	1024	10
Cifar100	50000	512	100
Fashion	60000	1280	10
YTF20	63896	512	20

Table 1: Datasets description.

B , which incurs a cost of $O(B^2)$. During the computation of the NNC score, the Hungarian matching algorithm introduces an additional complexity of $O(K^3)$. Therefore, the total time complexity is $O(K \log K + K + B^2 + K^3)$. As for space complexity, the nearest neighbor index requires $O(K)$ space, the adjacency matrix occupies $O(K^2)$, and the distance matrix within each mini-batch takes $O(B^2)$. In addition, constructing the confusion matrix for computing the NNC score requires $O(K^2)$ space. Consequently, the overall space complexity is $O(K + 2K^2 + B^2)$.

Experiments

Experimental Setup

Regarding the datasets, we employ eight single-view datasets: MSRCv1¹, HW2², Wiki³, MNIST⁴, Cifar10⁵, Cifar100⁶, Fashion (Xiao, Rasul, and Vollgraf 2017), YTF20⁷, as shown in Table 1. Regarding the comparison methods, since the proposed algorithm addresses the issue of K -value selection in parameter-free clustering, we select nine Non- K clustering methods: FINCH (Sarfraz, Sharma, and Stiefelhaugen 2019), COMIC (Peng et al. 2019), BP (Averbuch-Elor, Bar, and Cohen-Or 2020), DenMune (Abbas, El-Zoghabi, and Shoukry 2021), DeepDPM (Ronen, Finder, and Freifeld 2022), MPAASL (Dai et al. 2024), TC (Yang and Lin 2025), Gauging- δ (Yao, Pan, and Zeng 2025) and AFCL (Zhang et al. 2025b). Moreover, we also selected two Given- K methods for reference comparison: DCGL (Chen, Wang, and Li 2024) and DMAC (Wang et al. 2025). Finally, we adopt four metrics to evaluate clustering quality: Accuracy (ACC), Normalized Mutual Information (NMI), Purity (PUR), and F-score. More information about the datasets, comparison methods, and implementation details is provided in the Appendix.

Clustering Performance Comparison

As shown in Table 2, 3, SCMax demonstrates superior clustering performance. Compared with Non- K clustering

¹<https://www.microsoft.com/en-us/research/project/image-understanding>

²<https://cs.nyu.edu/roweis/data.html>

³<http://www.svcl.ucsd.edu/projects/crossmodal/>

⁴<http://yann.lecun.com/exdb/mnist/>

⁵<http://www.cs.toronto.edu/~kriz/cifar.html>

⁶<http://www.cs.toronto.edu/~kriz/cifar.html>

⁷<https://www.cs.tau.ac.il/~wolf/ytfaces/>

Datasets	FINCH CVPR'19	COMIC ICML'19	BP TPAMI'20	DenMune PR'21	DeepDPM CVPR'22	MPAASL ICML'24	TC TPAMI'25	Gauging- δ TPAMI'25	AFCL AAAI'25	SCMax
ACC										
MSRCv1	0.2524	0.1667	0.2762	0.4048	0.1429	0.4476	0.3048	0.2333	0.0310	0.6238
HW2	0.1975	0.1045	0.1410	0.2005	0.1000	0.5980	0.4725	0.1000	0.0005	0.6115
Wiki	0.5286	0.1207	0.4833	0.1019	0.1574	0.5056	0.4682	0.1574	0.0052	0.5967
MNIST	0.1968	0.1028	0.5004	0.0910	0.1000	0.5946	0.4752	0.1000	0.1000	0.6004
Cifar10	0.7117	OOM	OOM	0.0193	0.8178	OOM	OOM	OOM	OOM	0.8703
Cifar100	0.5999	OOM	OOM	0.0742	0.3100	OOM	OOM	OOM	OOM	0.9061
Fashion	0.2933	OOM	OOM	0.0183	0.3652	OOM	OOM	OOM	OOM	0.7542
YTF20	0.1238	OOM	OOM	0.0253	0.4890	OOM	OOM	OOM	OOM	0.6493
NMI										
MSRCv1	0.2185	0.0454	0.1335	0.5479	0.0000	0.5888	0.5567	0.0986	0.2936	0.5597
HW2	0.3480	0.0128	0.0731	0.5616	0.0000	0.7459	0.5998	0.0000	0.2198	0.6436
Wiki	0.5448	0.4654	0.5209	0.4151	0.0000	0.5322	0.5284	0.0000	0.0061	0.5609
MNIST	0.3562	0.0109	0.6005	0.4946	0.0000	0.7385	0.6321	0.0000	0.0000	0.7021
Cifar10	0.7262	OOM	OOM	0.3707	0.7474	OOM	OOM	OOM	OOM	0.7714
Cifar100	0.8246	OOM	OOM	0.6712	0.8368	OOM	OOM	OOM	OOM	0.9801
Fashion	0.4830	OOM	OOM	0.3587	0.6511	OOM	OOM	OOM	OOM	0.7479
YTF20	0.0503	OOM	OOM	0.4490	0.8126	OOM	OOM	OOM	OOM	0.8065
PUR										
MSRCv1	0.2524	0.1667	0.2810	0.6762	0.1429	0.7762	0.7905	0.2333	0.5262	0.6476
HW2	0.1975	0.1065	0.1410	0.8625	0.1000	0.6960	0.7785	0.1000	0.2295	0.6115
Wiki	0.6350	0.9337	0.6308	0.6933	0.1574	0.6497	0.6643	0.1574	0.2102	0.6403
MNIST	0.1968	0.1052	0.5004	0.8708	0.1000	0.8738	0.8228	0.1000	0.2178	0.7658
Cifar10	0.7117	OOM	OOM	0.8361	0.8376	OOM	OOM	OOM	OOM	0.8922
Cifar100	0.5999	OOM	OOM	0.9055	0.3100	OOM	OOM	OOM	OOM	0.9318
Fashion	0.2933	OOM	OOM	0.8161	0.8358	OOM	OOM	OOM	OOM	0.8497
YTF20	0.1238	OOM	OOM	0.8345	0.9711	OOM	OOM	OOM	OOM	0.8071
F-score										
MSRCv1	0.1593	0.0803	0.2029	0.2045	0.0357	0.2066	0.0797	0.1322	0.4419	0.5698
HW2	0.0738	0.0247	0.0799	0.0234	0.0182	0.5175	0.2430	0.0182	0.2695	0.5538
Wiki	0.3957	0.0011	0.3574	0.0069	0.0272	0.2895	0.2534	0.0272	0.1822	0.5538
MNIST	0.0741	0.0121	0.4255	0.0035	0.0182	0.3603	0.2318	0.0182	0.1540	0.4553
Cifar10	0.6484	OOM	OOM	0.0001	0.7933	OOM	OOM	OOM	OOM	0.8001
Cifar100	0.5778	OOM	OOM	0.0029	0.1691	OOM	OOM	OOM	OOM	0.8476
Fashion	0.1854	OOM	OOM	0.0000	0.1550	OOM	OOM	OOM	OOM	0.6187
YTF20	0.0332	OOM	OOM	0.0001	0.1543	OOM	OOM	OOM	OOM	0.5671

Table 2: Non- K methods clustering performance comparison results, where the best results are highlighted in bold and OOM denotes out of memory error.

methods, it achieves the highest scores in both ACC and F-score across all datasets, indicating its strong capability to uncover the true underlying cluster structures. For the NMI metric, SCMax also exhibits robust performance, significantly outperforming most competitors. Although it does not always achieve the best NMI on a few datasets such as MSRCv1, its results remain very close to the top-performing method, confirming its adaptability and effectiveness across diverse application scenarios. Meanwhile, for the PUR metric—which often favors over-segmentation—SCMax still delivers competitive results, reflecting its balanced performance across multiple evaluation perspectives. Compared with Given- K clustering methods, it is important to note that such a comparison is inherently unfair: Given- K methods operate with the prior knowledge of the cluster number K , whereas Non- K methods must simultaneously per-

form cluster number estimation and clustering optimization, incurring additional K -value selection overhead. Even under this unfair comparison, our method still achieves highly competitive results and even attains the best performance on several datasets, including Wiki, Cifar10, Cifar100, Fashion, and YTF20. Overall, these results strongly validate the effectiveness and robustness of SCMax in practical tasks.

Due to the page limitation, the comparisons of estimated cluster number, running time and computational complexity for all methods are provided in the Appendix.

Ablation Study

To evaluate the effectiveness and design rationale of each component in SCMax, we conducted ablation studies. Table 4 reports the ACC scores on four representative datasets, complete results are provided in the Appendix. We designed

Methods	MSRCv1	HW2	Wiki	MNIST	Cifar10	Cifar100	Fashion	YTF20
ACC								
DCGL (AAAI'24)	0.6810	0.6185	0.5534	0.6246	OOM	OOM	OOM	OOM
DMAC (AAAI'25)	0.4905	0.5285	0.1574	0.1000	OOM	OOM	OOM	OOM
SCMax	0.6238	0.6115	0.5967	0.6004	0.8703	0.9061	0.7542	0.6493
NMI								
DCGL (AAAI'24)	0.6143	0.6804	0.5356	0.6621	OOM	OOM	OOM	OOM
DMAC (AAAI'25)	0.4841	0.4708	0.0000	0.0000	OOM	OOM	OOM	OOM
SCMax	0.5597	0.6436	0.5609	0.7021	0.7714	0.9801	0.7479	0.8065
PUR								
DCGL (AAAI'24)	0.7000	0.6940	0.6179	0.6712	OOM	OOM	OOM	OOM
DMAC (AAAI'25)	0.5381	0.5425	0.1574	0.1000	OOM	OOM	OOM	OOM
SCMax	0.6476	0.6115	0.6403	0.7658	0.8922	0.9318	0.8497	0.8071
F-score								
DCGL (AAAI'24)	0.6771	0.5322	0.5428	0.6206	OOM	OOM	OOM	OOM
DMAC (AAAI'25)	0.3776	0.5349	0.0272	0.0182	OOM	OOM	OOM	OOM
SCMax	0.5698	0.5538	0.5538	0.4553	0.8001	0.8476	0.6187	0.5671

Table 3: Given- K methods clustering performance comparison results, where the best results are highlighted in bold and OOM denotes out of memory error.

Datasets	SCMax	Remove CL - I	Remove CL - II	Select Random Noise	Choose \mathbf{G}' as result
MSRCv1	0.6238	0.6238	0.6238	0.1429	0.4952
MNIST	0.6004	0.3158	0.3902	0.6004	0.5596
Fashion	0.7542	0.1980	0.3913	0.7542	0.7194
YTF20	0.6493	0.2071	0.6493	0.3421	0.6455

Table 4: The ablation experiment results on four representative datasets are presented, only showing the ACC metric results. The best result is displayed in bold. The complete results can be found in the Appendix.

four ablation settings:

- Remove CL-I: Removing the contrastive learning constraint Part I, retaining only the perturbation method based on pushing apart negative (different-class) samples.
- Remove CL-II: Removing the contrastive learning constraint Part II, retaining only the perturbation method based on pulling together positive (same-class) samples.
- Select Random Noise: Replacing perturbation with random noise sampled from $[-1, 1]$, whose standard deviation matches that of the fixed representation \mathbf{Z} .
- Choose \mathbf{G}' as Result: Selecting the cluster structure \mathbf{G}' at the moment of consensus maximization as the final result.

Experimental results show that removing or replacing any component leads to performance degradation, validating the necessity of each design. Notably, the comparison between "Remove CL-I" and "Remove CL-II" indicates that perturbations based on pushing apart negative samples have a more pronounced impact, suggesting that negative pair repulsion plays a more critical role in generating effective perturbations. The "Select Random Noise" setting leads to unstable and highly variable results, revealing the limitations of perturbations without structural constraints. Moreover, the "Choose \mathbf{G}' as Result" setting consistently yields inferior performance compared to choosing \mathbf{G} , further indi-

cating that the perturbed candidate cluster structures are less likely to produce optimal clustering results.

Analysis

In this subsection, we analyze SCMax from two perspectives: **the NNC score** and **loss convergence**. The NNC score effectively evaluates the latent cluster structure, reaching its maximum exactly at the closest ground-truth number of clusters, while SCMax exhibits stable and efficient training, with both the autoencoder and contrastive losses showing steady convergence. For details, see the Appendix.

Conclusion

The proposed SCMax framework addresses the true parameter-free clustering problem. By integrating hierarchical clustering, self-supervised representation learning, and nearest-neighbor-based consensus evaluation within a unified process, SCMax not only dynamically guides the generation of clustering number but also automatically evaluates the optimal clustering structure. Extensive experimental results demonstrate the superior performance of SCMax across multiple datasets. In future work, we aim to explore more advanced cluster number generation strategies to further enhance the accuracy and robustness of the resulting clustering structures. Furthermore, we plan to eliminate the reliance of the autoencoder-based representation learning module on predefined architectural structures.

Appendix

Details of Employed Datasets

This section provides detailed descriptions of the eight datasets used in our experiments.

- MSRCv1: An image segmentation and object recognition dataset containing multiple semantic object categories.
- HW2: A handwritten digit image dataset containing multiple digit categories.
- Wiki: A multimodal dataset containing multiple semantic topic categories.
- MNIST: A heterogeneous multi-view handwritten digit dataset containing multiple digit categories.
- Cifar10: A natural image dataset containing multiple common object categories.
- Cifar100: A fine-grained version of the Cifar10 dataset containing multiple specific object subcategories.
- Fashion: A fashion image dataset containing multiple clothing categories.
- YTF20: A face image dataset containing multiple identity categories.

Details of Comparison Methods

This section provides detailed descriptions of the eleven comparison methods employed in our experiments.

- FINCH: A Non- K hierarchical clustering algorithm based on nearest neighbors, capable of generating cluster partitions at different levels. Since this method does not provide an evaluation mechanism for partition selection, we choose the clustering number corresponding to the last partition as the final result.
- COMIC: A Non- K multi-view clustering method that integrates geometric consistency and clustering assignment consistency, achieving efficient clustering without predefining the number of clusters. Moreover, we follow the original paper’s setting and use the average length of the shortest 90% similarity graph edges as the threshold for final cluster structure formation.
- BP: A Non- K clustering method that explicitly reveals the core cluster structure by progressively peeling off boundary points. For fairness, we follow the original paper’s autoencoder configuration, reducing features to 10 dimensions and training for 100 epochs. Other parameter settings are in accordance with the open-source code of the original paper.
- DenMune: A Non- K clustering method based on neighbor density consistency. The paper indicates the method is insensitive to hyperparameters, thus, we set the number of k -nearest neighbors to 4 during reproduction, consistent with the original paper’s demo dataset setting.
- DeepDPM: A deep Non- K clustering method based on a split-merge strategy that can automatically infer the number of clusters during training. Following the settings of

the original paper, we use the same autoencoder architecture as SCMax, train for 200 epochs, reduce the feature dimensions to 128, and set the initial number of clusters to the default value of 1.

- MPAASL: A Non- K multi-view clustering method combining graph consistency modeling with reinforcement learning mechanisms. We obtained the source code by contacting the authors and set the view voting mechanism to “all” during reproduction.
- TC: A Non- K clustering method based on an automatic merge strategy guided by inter-cluster mass and distance, which can adaptively discover the cluster structure without predefining the cluster number. All parameter settings are in accordance with the open-source code of the original paper.
- Gauging- δ : A Non- K clustering method based on an adaptive merge strategy. The method introduces a gauging function that leverages statistical and environmental information of clusters to adaptively determine whether two clusters can be merged. Following the original paper, We employed a simulated CNN architecture to reduce the features to 128 dimensions.
- AFCL: A Non- K federated clustering method designed for asynchronous and heterogeneous client scenarios. The method introduces redundant seed points as communication media and gradually prunes them to reveal the global cluster distribution without requiring the true number of clusters. In reproduction, we followed the original settings: we removed the missing samples and normalized all the data.
- DMAC: A Given- K multi-view clustering method based on learnable anchors. Unlike traditional approaches with fixed anchors, DMAC employs noise-driven anchor learning and anchor graph convolution, ensuring anchors adapt during training.
- DCGL: A Given- K clustering method combining autoencoder and graph convolution with dual contrastive guidance. The method enhances discriminability by integrating feature-level contrast and cluster-level contrast, jointly optimizing both original features and learned graph structures.

For SCMax, the architecture of the autoencoder is: $\text{dim}(X)$ -500-500-2000-256. The autoencoder is trained for 200 epochs, with 50 epochs for contrastive learning constraints in each round. We set the batch size to 256, learning rate to 0.0003, and the random seed to 3407 (Picard 2021). Moreover, all experiments are conducted on a machine configured with 60 GB of RAM, a 16 vCPU AMD EPYC 9654 processor (96 cores), and a virtual GPU with 32 GB of VRAM⁸.

⁸<https://www.autodl.com/home>

Methods	MSRCv1	HW2	Wiki	MNIST	Cifar10	Cifar100	Fashion	YTF20
K_{true}	7	10	10	10	10	100	10	20
FINCH	2	2	13	2	8	60	3	2
COMIC	3	6	1786	20	OOM	OOM	OOM	OOM
BP	3	2	15	6	OOM	OOM	OOM	OOM
DenMune	19	138	247	450	5224	4590	6206	7491
DeepDPM	1	1	1	1	11	31	33	86
MPAASL	19	11	19	19	OOM	OOM	OOM	OOM
TC	37	24	21	26	OOM	OOM	OOM	OOM
Gauging- δ	4	1	1	1	OOM	OOM	OOM	OOM
AFCL	7	18	10	10	OOM	OOM	OOM	OOM
DCGL	—	—	—	—	—	—	—	—
DMAC	—	—	—	—	—	—	—	—
SCMax	8	8	10	15	11	106	13	25

Table 5: Estimated number of clusters by each method, where the result closest to the ground truth is highlighted in bold.

Methods	MSRCv1	HW2	Wiki	MNIST	Cifar10	Cifar100	Fashion	YTF20
FINCH	0.03	0.11	0.12	0.48	23.52	22.28	30.73	37.18
COMIC	2.71	24.30	32.61	166.69	OOM	OOM	OOM	OOM
BP	<i>0.10</i>	2.50	<i>4.41</i>	13.12	OOM	OOM	OOM	OOM
DenMune	0.62	3.78	5.34	10.04	<i>141.44</i>	<i>132.72</i>	<i>183.61</i>	<i>173.84</i>
DeepDPM	629.19	656.86	682.84	745.03	4044.09	6554.37	8269.58	12128.43
MPAASL	257.05	3511.38	6340.23	16718.54	OOM	OOM	OOM	OOM
TC	1.15	<i>0.84</i>	21.50	<i>3.66</i>	OOM	OOM	OOM	OOM
Gauging- δ	5.73	3311.67	3573.84	38974.31	OOM	OOM	OOM	OOM
AFCL	539.85	2925.35	293.47	9276.38	OOM	OOM	OOM	OOM
DCGL	7.49	303.30	742.11	3209.28	OOM	OOM	OOM	OOM
DMAC	7.59	18.87	26.22	48.82	OOM	OOM	OOM	OOM
SCMax	4.94	16.86	14.46	43.41	1168.78	1163.23	1821.79	1052.95

Table 6: Running time of each method, where the shortest running time is highlighted in bold and the second shortest is shown in italics.

Method	Memory Cost	Time Complexity	Max Reported
FINCH	$O(N)$	$O(N \log N)$	63896
COMIC	$O(N^2)$	$O(N^2)$	5000
BP	$O(ND)$	$O(N^2)$	5000
DenMune	$O(NK)$	$O(N^2K)$	63896
DeepDPM	$O(NK)$	$O(NKD^2)$	63896
MPAASL	$O(N^2)$	$O(N^3)$	5000
TC	$O(N^2)$	$O(N \log N)$	5000
Gauging- δ	$O(N^2)$	$O(N^2 \log N)$	5000
AFCL	$O(ND)$	$O(KNDP)$	5000
DMAC	$O(ND)$	$O(NM)$	5000
DCGL	$O(N^2)$	$O(N^3)$	5000
SCMax	$O(K + 2K^2 + B^2)$	$O(K \log K + K + B^2 + K^3)$	63896

Table 7: The computational complexity of each method, where Max Reported denotes the maximum dataset size that can be processed, N represents the number of samples, M denotes the number of anchors, K is the number of clusters, B is the batch size, D is the feature dimension, and P is the number of clients.

Additional Comparisons of Clustering Performance

In this subsection, we present additional result analyses of our algorithm compared with eleven comparison methods across eight datasets. The supplementary analysis includes

the estimated number of clusters, the running time and the computational complexity.

Estimated Cluster Number Comparison. As shown in Table 5, SCMax achieves the most accurate estimation of the true number of clusters on most datasets, demonstrat-

Datasets	SCMax	Remove CL - I	Remove CL - II	Select Random Noise	Choose G' as result
ACC					
MSRCv1	0.6238	0.6238	0.6238	0.1429	0.4952
HW2	0.6115	0.5115	0.2955	0.2955	0.6465
Wiki	0.5976	0.3814	0.5967	0.5967	0.5963
MNIST	0.6004	0.3158	0.3902	0.6004	0.5596
Cifar10	0.8703	0.2458	0.8703	0.8703	0.8261
Cifar100	0.9061	0.9061	0.9061	0.9061	0.8480
Fashion	0.7542	0.1980	0.3913	0.7542	0.7194
YTF20	0.6493	0.2071	0.6493	0.3421	0.6455
NMI					
MSRCv1	0.5597	0.5597	0.5597	0.0000	0.4881
HW2	0.6436	0.6574	0.5329	0.5329	0.6992
Wiki	0.5609	0.5100	0.5609	0.5609	0.5528
MNIST	0.7021	0.6436	0.5703	0.7021	0.7059
Cifar10	0.7714	0.5507	0.7714	0.7714	0.7489
Cifar100	0.9801	0.9801	0.9801	0.9801	0.9690
Fashion	0.7479	0.5352	0.6084	0.7479	0.7131
YTF20	0.8605	0.7031	0.8065	0.5535	0.7982
PUR					
MSRCv1	0.6476	0.6476	0.6476	0.1429	0.6000
HW2	0.6115	0.8065	0.2955	0.2955	0.6465
Wiki	0.6403	0.6647	0.6403	0.6403	0.6270
MNIST	0.7658	0.8970	0.3902	0.7658	0.8370
Cifar10	0.8922	0.8961	0.8922	0.8922	0.8824
Cifar100	0.9318	0.9318	0.9318	0.9318	0.9287
Fashion	0.8497	0.8696	0.3913	0.8497	0.8355
YTF20	0.8071	0.9842	0.8071	0.3421	0.8269
F-score					
MSRCv1	0.5698	0.5698	0.5698	0.0357	0.3821
HW2	0.5538	0.2588	0.1377	0.1377	0.5473
Wiki	0.5538	0.1641	0.5538	0.5538	0.5424
MNIST	0.4553	0.0901	0.2580	0.4553	0.3552
Cifar10	0.8001	0.0256	0.8001	0.8001	0.7170
Cifar100	0.8476	0.8476	0.8476	0.8476	0.6646
Fashion	0.6178	0.0168	0.2451	0.6178	0.5465
YTF20	0.5671	0.0267	0.5671	0.1671	0.5368

Table 8: The complete ablation experiment results, including four evaluation indicators: ACC, NMI, PUR, and F-score. The best result is displayed in bold.

Datasets	K_{true}	SCMax	Remove CL - I	Remove CL - II	Select Random Noise	Choose G' as result
MSRCv1	7	8	8	8	1	10
HW2	10	8	24	3	3	7
Wiki	10	10	28	10	10	9
MNIST	10	15	51	4	15	19
Cifar10	10	11	148	11	11	12
Cifar100	100	106	106	106	106	129
Fashion	10	13	190	4	13	14
YTF20	20	25	262	25	6	27

Table 9: The ablation experiment results of the number of clusters predicted by all methods. The best result is displayed in bold.

ing its superior capability in cluster number inference. Notably, on large-scale datasets with over ten thousand samples, SCMax significantly outperforms other methods. This advantage stems from its parameter-free and efficient unified framework, enabling it to better adapt to complex high-

dimensional data. By contrast, other methods show various limitations: FINCH and BP lack effective evaluation mechanisms and tend to produce trivial solutions, grouping most samples into a single cluster. COMIC, DenMune, and TC are overly dependent on sensitive explicit or implicit thresh-

Datasets	SCMax	Remove CL - I	Remove CL - II	Select Random Noise	Choose G' as result
MSRCv1	4.94	5.06	4.96	4.48	4.94
HW2	16.86	14.84	17.99	9.87	16.86
Wiki	14.46	17.59	17.43	10.31	14.46
MNIST	43.41	38.25	42.51	21.33	43.41
Cifar10	1168.78	1128.83	1202.92	955.88	1168.78
Cifar100	1163.23	1122.84	1165.80	1014.40	1163.23
Fashion	1821.79	1720.86	1817.21	1508.49	1821.79
YTF20	1052.95	1049.76	1104.84	816.60	1052.95

Table 10: The ablation experiment results of the running times for all methods. The best result is displayed in bold.

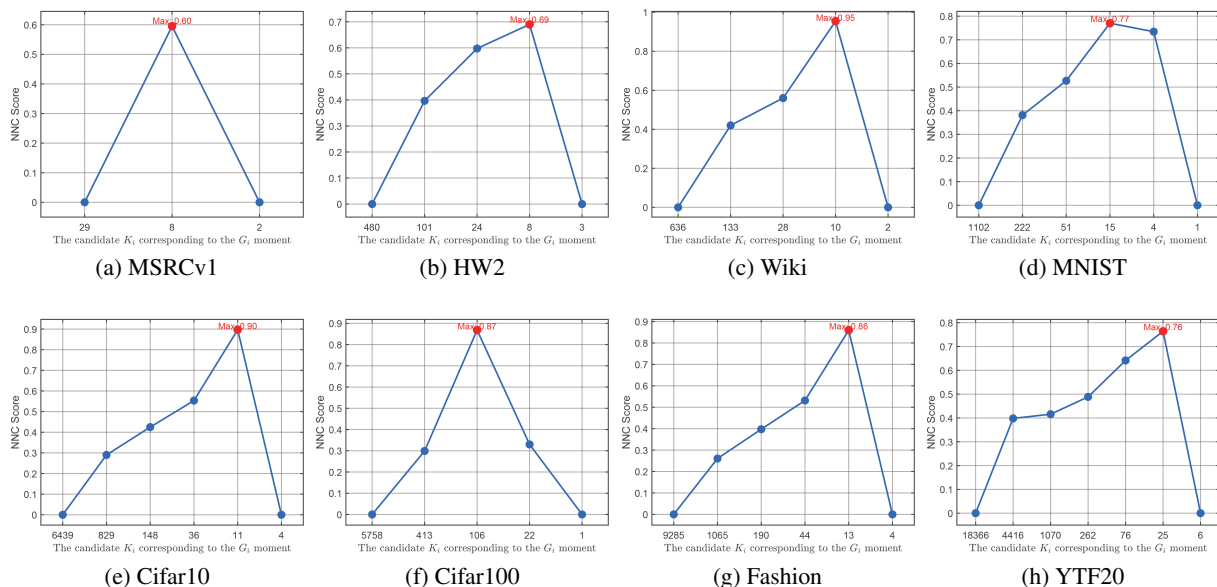


Figure 3: The NNC scores of the candidate K_i values corresponding to the G_i time on all datasets.

old parameters, which, if misconfigured, lead to local optima and oversegmentation. DeepDPM requires an initial number of clusters; inaccurate initialization can misguide the entire clustering process, especially on small datasets. MPAASL restricts the search space to a predefined range of K , limiting its generalizability beyond the specified range.

Running Time Comparison. As shown in Table 6, SCMax not only estimates cluster numbers accurately but also delivers outstanding computational efficiency. On all datasets, its runtime remains highly competitive, particularly on large-scale datasets, where it completes clustering in a short time, showcasing strong scalability. In contrast, comparison methods present various computational challenges: DeepDPM incurs high training time due to its complex deep modeling. COMIC, BP, MPAASL, TC, DCFL, and DMAC frequently experience out-of-memory (OOM) issues due to high computational demands. FINCH often shows extremely low runtime because it simply selects the last candidate K as the final result due to its lack of an effective evaluation mechanism. DenMune frequently stops early due to its sensitivity to improper threshold settings, leading

to oversegmentation and relatively low computational cost.

Computational Complexity Comparison. As shown in Table 7, SCMax achieves highly competitive computational complexity while maintaining optimal clustering performance. First, compared with Non- K clustering methods, the complexity of SCMax mainly depends on the number of clusters K and the batch size B , rather than the total number of samples N or the feature dimension D . This design enables SCMax to scale effectively to large datasets. In contrast, most Non- K methods (such as COMIC, BP, MPAASL, TC, Gauging- δ , and AFCL) exhibit quadratic or even cubic growth in complexity as N or D increases, leading to excessive memory consumption and frequent out-of-memory errors. Second, when compared with Given- K clustering methods, this comparison is inherently unfair: Given- K methods operate with the prior knowledge of the cluster number K , whereas Non- K methods must simultaneously perform cluster number estimation and clustering optimization, incurring additional K -value selection overhead. Even under such unfair conditions, SCMax still demonstrates lower overall complexity than Given- K methods such as

DCGL and DMAC. Notably, DCGL and DMAC can only run successfully on datasets with up to 5,000 samples, while they fail to operate on larger datasets containing tens of thousands of samples. In summary, SCMax maintains superior clustering performance while achieving remarkable computational efficiency and scalability.

Ablation Study on All Datasets

To further validate the stability and effectiveness of each component in the SCMax framework across different data environments, we supplement the appendix with four sets of ablation experiments conducted on all eight datasets. As shown in Tables 8, 9, and 10, all ablation settings exhibit a performance decline trend across different datasets, confirming the indispensable roles of each module in the overall framework. Besides the main results, some interesting observations can be made: First, although ‘‘Select Random Noise’’ as a perturbation method shows very unstable performance, occasionally good results inspire us to simplify the perturbation strategy in future designs, indicating potential computational efficiency gains. Second, the results from ‘‘Choose G' as result’’ demonstrate that the cluster number evaluation can only accurately identify the best candidate K but cannot evaluate cluster numbers outside the candidate set. Therefore, clustering performance depends solely on the quality of candidate K 's generated by the cluster number generation module, which guides future explorations towards higher-quality cluster number generation strategies.

NNC Score Analysis

In this section, we visualize the NNC scores corresponding to the candidate cluster structures G_i at different moments and investigate the reliability of the nearest-neighbor consensus evaluation. As illustrated in Figure 3, the variation of the NNC score shows that as K_i approaches the true number of clusters, the NNC score increases steadily, and it decreases as the estimated number moves further away from the ground truth. This verifies the effectiveness of nearest-neighbor consensus in evaluating cluster structure. Remarkably, the Maximum of the NNC score aligns precisely with the closest ground-truth cluster structure, indicating that the metric can accurately identify the optimal number of clusters without any hyperparameter settings. These results show our metric can adaptively and reliably estimate data’s intrinsic structure without any parameters.

Convergence Analysis

To analyze the convergence of SCMax, we track the loss values during training on Cifar10 and Cifar100 as the number of iterations increases. As shown in Figure 4, the proposed SCMax exhibits a clear convergence trend. The total loss consists of two parts: the loss L_R from the autoencoder (AE) and the loss L_Q from contrastive learning (CL) constraints. Both losses consistently decrease throughout training, indicating continuous improvement in dimensionality reduction and feature optimization. Specifically, the autoencoder loss drops rapidly in the early stages, demonstrating that the model quickly captures the basic structure of the

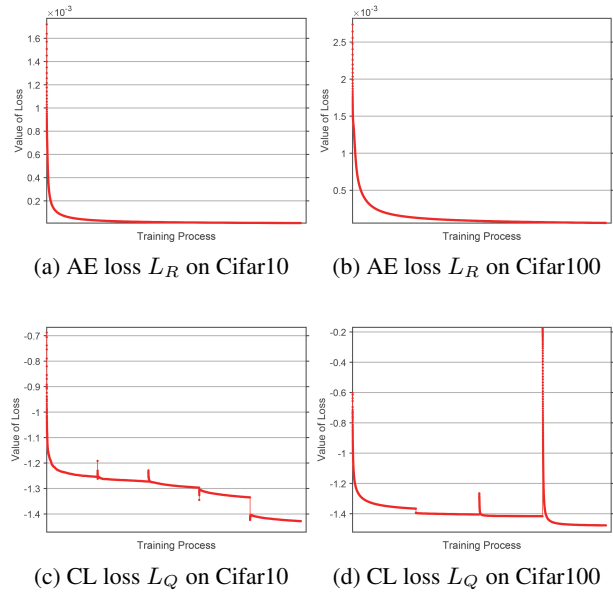


Figure 4: Convergence curves on the Cifar10 and Cifar100 datasets. Here, each iteration represents one time of network training, including both the autoencoder and contrastive learning constraints.

data. Meanwhile, the contrastive learning loss also decreases and stabilizes across different candidate K values, showing the model’s persistent ability to enhance feature discriminability. Overall, SCMax demonstrates a smooth and efficient training process across both datasets, further validating the soundness and effectiveness of its training strategy.

Acknowledgements

This work is supported by the National Science Fund for Distinguished Young Scholars of China (No. 62325604), and the National Natural Science Foundation of China (No. 62276271 and 62376039).

References

Abbas, M.; El-Zoghabi, A.; and Shoukry, A. 2021. Den-Mune: Density peak based clustering using mutual nearest neighbors. *Pattern Recognition*, 109: 107589.

Averbuch-Elor, H.; Bar, N.; and Cohen-Or, D. 2020. Border-Peeling Clustering. *IEEE Transactions on Pattern Analysis and Machine Intelligence*, 42(07): 1791–1797.

Bagirov, A. M.; Aliguliyev, R. M.; and Sultanova, N. 2023. Finding compact and well-separated clusters: Clustering using silhouette coefficients. *Pattern Recognition*, 135: 109144.

Chen, M.; Wang, B.; and Li, X. 2024. Deep contrastive graph learning with clustering-oriented guidance. In *Proceedings of the AAAI Conference on Artificial Intelligence*, volume 38, 11364–11372.

- Dai, H.; Liu, Y.; Su, P.; Cai, H.; Huang, S.; and Lv, J. 2024. Multi-view clustering by inter-cluster connectivity guided reward. In *International Conference on Machine Learning*.
- Dang, Z.; Deng, C.; Yang, X.; Wei, K.; and Huang, H. 2021. Nearest neighbor matching for deep clustering. In *Proceedings of the IEEE/CVF Conference on Computer Vision and Pattern Recognition*, 13693–13702.
- He, W.; Wang, Z.; and Zhang, Y. 2025. Target Semantics Clustering via Text Representations for Robust Universal Domain Adaptation. In *Proceedings of the AAAI Conference on Artificial Intelligence*, volume 39, 17132–17140.
- Kodinariya, T.; and Makwana, P. 2013. Review on Determining of Cluster in K-means Clustering. *International Journal of Advance Research in Computer Science and Management Studies*, 1: 90–95.
- Li, D.; Zhou, S.; Zeng, T.; and Chan, R. H. 2024. Multi-Prototypes Convex Merging Based K-Means Clustering Algorithm. *IEEE Transactions on Knowledge and Data Engineering*, 36(11): 6653–6666.
- Liu, S.; Zhang, J.; Wen, Y.; Yang, X.; Wang, S.; Zhang, Y.; Zhu, E.; Tang, C.; Zhao, L.; and Liu, X. 2024. Sample-level cross-view similarity learning for incomplete multi-view clustering. In *Proceedings of the AAAI conference on Artificial Intelligence*, volume 38, 14017–14025.
- Liu, Y.; Liang, K.; Xia, J.; Yang, X.; Zhou, S.; Liu, M.; Liu, X.; and Li, S. Z. 2023. Reinforcement graph clustering with unknown cluster number. In *Proceedings of the ACM International Conference on Multimedia*, 3528–3537.
- Peng, X.; Huang, Z.; Lv, J.; Zhu, H.; and Zhou, J. T. 2019. COMIC: Multi-view clustering without parameter selection. In *International Conference on Machine Learning*, 5092–5101. PMLR.
- Picard, D. 2021. Torch. manual_seed (3407) is all you need: On the influence of random seeds in deep learning architectures for computer vision. *arXiv preprint arXiv:2109.08203*.
- Qin, Y.; and Qian, L. 2024. Fast elastic-net multi-view clustering: a geometric interpretation perspective. In *Proceedings of the 32nd ACM international conference on multimedia*, 10164–10172.
- Qiu, L.; Zhang, Q.; Chen, X.; and Cai, S. 2024. Multi-level cross-modal alignment for image clustering. In *Proceedings of the AAAI Conference on Artificial Intelligence*, volume 38, 14695–14703.
- Rodriguez, A.; and Laio, A. 2014. Clustering by fast search and find of density peaks. *science*, 344(6191): 1492–1496.
- Ronen, M.; Finder, S. E.; and Freifeld, O. 2022. Deepdpm: Deep clustering with an unknown number of clusters. In *Proceedings of the IEEE/CVF Conference on Computer Vision and Pattern Recognition*, 9861–9870.
- Sarfraz, S.; Sharma, V.; and Stiefelwagen, R. 2019. Efficient parameter-free clustering using first neighbor relations. In *Proceedings of the IEEE/CVF Conference on Computer Vision and Pattern Recognition*, 8934–8943.
- Schubert, E. 2023. Stop using the elbow criterion for k-means and how to choose the number of clusters instead. *ACM SIGKDD Explorations Newsletter*, 25(1): 36–42.
- Shah, S. A.; and Koltun, V. 2017. Robust continuous clustering. *Proceedings of the National Academy of Sciences*, 114(37): 9814–9819.
- Shi, C.; Wei, B.; Wei, S.; Wang, W.; Liu, H.; and Liu, J. 2021. A quantitative discriminant method of elbow point for the optimal number of clusters in clustering algorithm. *EURASIP Journal on Wireless Communications and Networking*, 2021(1): 31.
- Sun, L.; Huang, Z.; Peng, H.; Wang, Y.; Liu, C.; and Yu, P. S. 2024. LSEnet: Lorentz structural entropy neural network for deep graph clustering. In *International Conference on Machine Learning*, 47078–47104.
- Wang, B.; Zeng, C.; Chen, M.; and Li, X. 2025. Towards Learnable Anchor for Deep Multi-View Clustering. In *Proceedings of the AAAI Conference on Artificial Intelligence*, volume 39, 21044–21052.
- Wang, F.; Jin, J.; Hu, J.; Liu, S.; Yang, X.; Wang, S.; Liu, X.; and Zhu, E. 2024. Evaluate then cooperate: Shapley-based view cooperation enhancement for multi-view clustering. *Advances in Neural Information Processing Systems*, 37: 135355–135379.
- Wang, Z.; Ni, Y.; Jing, B.; Wang, D.; Zhang, H.; and Xing, E. 2022. DNB: A Joint Learning Framework for Deep Bayesian Nonparametric Clustering. *IEEE Transactions on Neural Networks and Learning Systems*, 33(12): 7610–7620.
- Xiao, A.; Chen, H.; Guo, T.; Zhang, Q.; and Wang, Y. 2023. Deep Plug-and-Play Clustering with Unknown Number of Clusters. *Transactions on Machine Learning Research*.
- Xiao, H.; Rasul, K.; and Vollgraf, R. 2017. Fashion-MNIST: a Novel Image Dataset for Benchmarking Machine Learning Algorithms. *arXiv preprint arXiv:1708.07747*.
- Xing, Y.; He, T.; Xiao, T.; Wang, Y.; Xiong, Y.; Xia, W.; Wipf, D.; Zhang, Z.; and Soatto, S. 2021. Learning hierarchical graph neural networks for image clustering. In *Proceedings of the IEEE/CVF International Conference on Computer Vision*, 3467–3477.
- Yang, J.; and Lin, C.-T. 2025. Autonomous clustering by fast find of mass and distance peaks. *IEEE Transactions on Pattern Analysis and Machine Intelligence*.
- Yang, X.; Jing, H.; Zhang, Z.; Wang, J.; Niu, H.; Wang, S.; Lu, Y.; Wang, J.; Yin, D.; Liu, X.; et al. 2025. Darec: A disentangled alignment framework for large language model and recommender system. In *2025 IEEE 41st International Conference on Data Engineering (ICDE)*, 904–917. IEEE.
- Yang, X.; Yan, Y.; Huang, K.; and Zhang, R. 2019. Vsb-dvm: an end-to-end bayesian nonparametric generalization of deep variational mixture model. In *IEEE International Conference on Data Mining*, 688–697. IEEE.
- Yao, J.; Pan, J.; and Zeng, Y. 2025. Gauging-delta: A Non-parametric Hierarchical Clustering Algorithm. *IEEE Transactions on Pattern Analysis and Machine Intelligence*.
- Yu, S.; Wang, S.; Dong, Z.; Tu, W.; Liu, S.; Lv, Z.; Li, P.; Wang, M.; and Zhu, E. 2024. A non-parametric graph clustering framework for multi-view data. In *Proceedings of the AAAI conference on Artificial Intelligence*, volume 38, 16558–16567.

Zhang, P.; Pan, Y.; Wang, S.; Yu, S.; Xu, H.; Zhu, E.; Liu, X.; and Tsang, I. 2025a. Max-Mahalanobis Anchors Guidance for Multi-View Clustering. In *Proceedings of the AAAI Conference on Artificial Intelligence*, volume 39, 22488–22496.

Zhang, Y.; Duan, Z.; Lu, M.; Ding, D.; Zhu, F.; and Ma, Z. 2024. Another way to the top: Exploit contextual clustering in learned image coding. In *Proceedings of the AAAI Conference on Artificial Intelligence*, volume 38, 9377–9386.

Zhang, Y.; Zhang, Y.; Lu, Y.; Li, M.; Chen, X.; and Cheung, Y.-m. 2025b. Asynchronous federated clustering with unknown number of clusters. In *Proceedings of the AAAI Conference on Artificial Intelligence*, volume 39, 22695–22703.

Zhao, H.; Yang, X.; and Deng, C. 2024. Parameter-agnostic deep graph clustering. *ACM Transactions on Knowledge Discovery from Data*, 18(3): 1–20.

Zhou, T.; Dong, Z.; Wang, S.; Liang, K.; Li, M.; Liu, X.; Zhu, E.; and Dong, X. 2025. DPFMVC: Dynamic Progressive Fusion for Multi-view Clustering. In *Proceedings of the 33rd ACM International Conference on Multimedia*, 1102–1111.